

Low energy neutral spectroscopy during pulsed discharge cleaning in PLT

D. Ruzic, S. Cohen, B. Denne, and J. Schivell

Citation: *J. Vac. Sci. Technol. A* 1, 818 (1983); doi: 10.1116/1.572002

View online: <http://dx.doi.org/10.1116/1.572002>

View Table of Contents: <http://avspublications.org/resource/1/JVTAD6/v1/i2>

Published by the AVS: Science & Technology of Materials, Interfaces, and Processing

Related Articles

Design and test of a magnetic shield for turbomolecular pumps

J. Vac. Sci. Technol. A 25, 1475 (2007)

Removal of carbon deposits in narrow gaps by oxygen plasmas at low pressure

J. Vac. Sci. Technol. A 25, 746 (2007)

High temperature outgassing tests on materials used in the DIII-D tokamak

J. Vac. Sci. Technol. A 24, 1572 (2006)

Retention of neon in graphite after ion beam implantation or exposures to the scrape-off layer plasma in the TEXTOR tokamak

J. Vac. Sci. Technol. A 20, 138 (2002)

Radio frequency siliconization: An approach to the coating for the future large superconducting fusion devices

J. Vac. Sci. Technol. A 19, 2149 (2001)

Additional information on *J. Vac. Sci. Technol. A*

Journal Homepage: <http://avspublications.org/jvsta>

Journal Information: http://avspublications.org/jvsta/about/about_the_journal


Top downloads: http://avspublications.org/jvsta/top_20_most_downloaded

Information for Authors: http://avspublications.org/jvsta/authors/information_for_contributors

ADVERTISEMENT


Instruments for advanced science

Gas Analysis



- dynamic measurement of reaction gas streams
- catalysis and thermal analysis
- molecular beam studies
- dissolved species probes
- fermentation, environmental and ecological studies

Surface Science




- UHV TPD
- SIMS
- end point detection in ion beam etch
- elemental imaging - surface mapping

Plasma Diagnostics



- plasma source characterization
- etch and deposition process reaction kinetic studies
- analysis of neutral and radical species

Vacuum Analysis



- partial pressure measurement and control of process gases
- reactive sputter process control
- vacuum diagnostics
- vacuum coating process monitoring

contact Hiden Analytical for further details

HIDEN ANALYTICAL

info@hideninc.com
www.HidenAnalytical.com

CLICK to view our product catalogue 

Low energy neutral spectroscopy during pulsed discharge cleaning in PLT

D. Ruzic, S. Cohen, B. Denne, and J. Schivell

Plasma Physics Laboratory, Princeton University, Princeton, New Jersey 08544

(Received 14 October 1982; accepted 13 December 1982)

The efflux of neutral hydrogen from PLT during discharge cleaning has been measured using a time-of-flight spectrometer. During high ionization pulsed discharge cleaning (PDC), the flux in the energy range of 5 to 1000 eV varies from 10^{14} $\text{H}^0/\text{cm}^2\cdot\text{s}$ to 10^{16} $\text{H}^0/\text{cm}^2\cdot\text{s}$ and the average energy from 10 to 80 eV. The energy distributions are nearly single temperature Maxwellians. Low ionization PDC (Taylor-type) produces a 1000 times lower fluence in the same energy range; however, a flux of 10^{16} $\text{H}^0/\text{cm}^2\cdot\text{s}$ at energies less than 5 eV is inferred. The detailed submillisecond time variation of these parameters with the fill gas pressure and state of cleanliness of the machine is presented. Comparisons with UV spectroscopy, bolometric measurements, and residual gas analysis are made.

PACS numbers: 52.55.Gb

I. INTRODUCTION

Plasma cleaning of vacuum vessels is a common and usually essential step in their preparation for UHV use. In tokamaks, pulsed discharge cleaning¹ (PDC) is the most prevalent method. On PLT, after an opening to air, nearly 10^5 PDC discharges are required before a 1 s duration high power tokamak discharge can be sustained.

The cleaning process is routinely monitored by mass spectrometric measurement of gases formed by the PDC discharges.^{2,3} The amount of impurities in the PDC plasma has been determined by UV spectroscopy⁴; and surface analysis³ has determined the cleanliness of materials exposed to PDC. These techniques do not fully answer the question of what causes the removal of impurities, predominantly C and O compounds, from the walls and limiters.

In the experiment described here, the flux and energy of the 5 to 1000 eV hydrogen atoms which hit the tokamak wall were measured. Their effectiveness in cleaning the wall and variations with machine cleanliness and fill pressure are discussed.

II. APPARATUS

The low energy neutral spectrometer⁵ (LENS) is a time-of-flight system which can measure the flux of H^0 between the energies of 5 and 1000 eV with a 0.25-ms-time resolution. The calibration below 30 eV was accomplished by extrapolating the flux from a measured 80-eV-Maxwellian distribution during startup of PLT and comparing it to the observed signal. An estimate of Franck-Condon dissociations and other possible signal sources were also included.⁶ The LENS views the plasma at its midplane 8.3° from normal. It is located near the top-bottom carbon limiters. A set of carbon ring limiters is 100° away toroidally.

A 1 m grazing incidence spectrometer⁷ with $\sim 1 \text{ \AA}$ resolution over a range of 40 to 1300 \AA and a time resolution of < 0.1 ms was used to study carbon and oxygen in the plasma. A platinum bolometer⁸ measured the total radiated power; and a quadrupole mass spectrometer was employed to study the gasses pumped out after the discharge.

III. PULSED CLEANING DISCHARGES

The cleaning plasmas were produced by the "pulse discharge cleaning electrical system."⁹ It discharges a 12 800- μF , 6-kV-capacitor bank through an ignitron into the Ohmic heating (OH) primary on PLT. In these experiments, the current I_{OH} passed through the OH primary in only one direction, i.e., the capacitor-coil circuit was not allowed to "ring."

There are two main types of cleaning discharges. The first has $\geq 95\%$ ionization and an input power of ~ 600 kW. It is called high ionization PDC. The second, called low ionization PDC, has only $\leq 2\%$ ionization and an input power ~ 60 kW. Low ionization PDC is similar to Taylor discharge cleaning.^{2,3} The parameter which determines the type of discharge is the fill pressure P_{fill} . High ionization discharges occur when $0.4 P_c \leq P_{\text{fill}} \leq P_c$, where P_c stands for the critical pressure. For $P_c \leq P_{\text{fill}} < 1.05 P_c$ low ionization discharges take place. Above $\sim 1.05 P_c$ and below $\sim 0.4 P_c$ no breakdown takes place. P_c is determined by the cleanliness of the machine. For a very dirty PLT, $P_c \approx 2 \times 10^{-4}$ T. After 5×10^4 PDC shots P_c is higher $\approx 3 \times 10^{-4}$ T. For a clean PLT, P_c is $\sim 4 \times 10^{-4}$ T.

IV. HIGH IONIZATION PDC

The I_{OH} , loop voltage (V_L), plasma current (I_p), pump duct pressure (P) from a calibrated ion gauge, and the line-averaged electron density (\bar{n}_e) from a 2-mm-microwave interferometer are shown in Fig. 1 for a typical high ionization PDC shot in a clean PLT. The ignitron was fired at $+23$ ms; the toroidal field was 2.32 kG.

In the absence of a plasma, $V_L = L(dI_{\text{OH}}/dt)$, where L is approximately the inductance linking the primary winding to the vacuum vessel. This basically holds except in region IV, where $I_{\text{OH}} = dI_{\text{OH}}/dt = 0$. In that region V_L is due to the plasma current alone. I_p and \bar{n}_e are initially a response to V_L . Though not noticeable on a scale shown in Fig. 1, I_p in region III is ~ -0.3 kA; and \bar{n}_e is $\sim 1 \times 10^{10} \text{ cm}^{-3}$. The duct pressure falls to its minimum, 5.5×10^{-5} Torr, at 0.12 s, about 30 ms after the PDC pulse. The calculated time con-

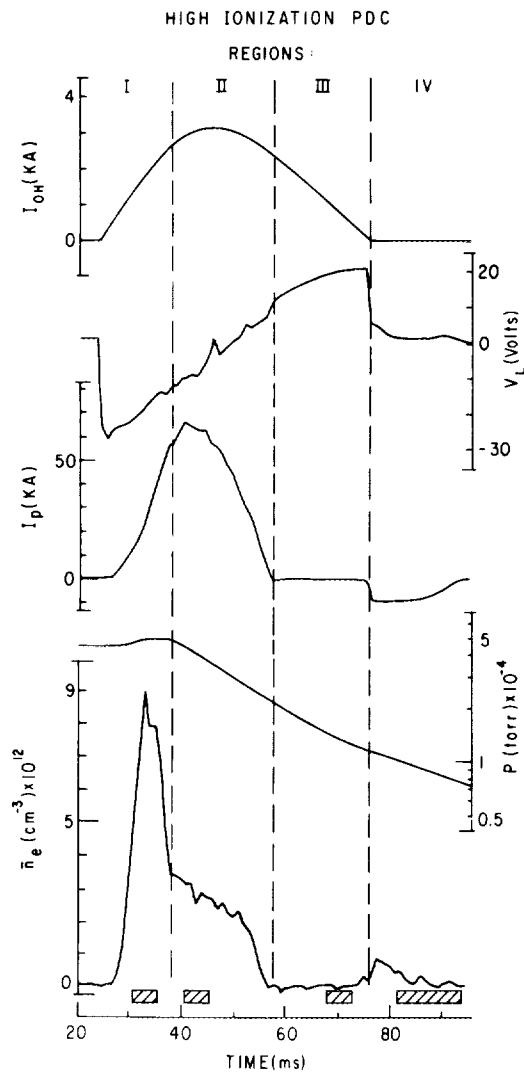


FIG. 1. Current in Ohmic heating primary (I_{OH}), loop voltage (V_L), plasma current (I_p), duct neutral pressure (P), and line average electron density (\bar{n}_e) vs time for high ionization PDC in a clean PLT. The toroidal field (TF) was 2.32 kG. The boxes represent the portions of the discharge averaged in Fig. 2. The four regions are discussed in the text.

stant due to the duct conductance is ~ 25 ms.

Energy spectra of the neutral H efflux during each of the four regions shown in Fig. 1 are presented in Fig. 2. The flux to 1000 eV was measured, although the displayed range is only to 150 eV. The portions of each region used to produce the energy spectra are shown graphically as boxes near the bottoms of Figs. 1, 3, and 4. The dots near each curve are a best fit to the data (by eye) of a Maxwellian distribution,

$$\frac{d\Gamma}{dE d\Omega} \propto \frac{1}{(T)^{3/2}} E e^{-E/T}. \quad (1)$$

The total incident flux Γ vs time is determined by integrating each individual energy spectrum over a specified energy range. Even for the hottest part of the discharge, region II, over 99% of the H^0 's have energies less than 400 eV. Figure 3 shows the total flux of H^0 with energies between 7.0 and 405 eV.

The neutral flux is produced by charge exchange and attenuated by electron impact ionization:

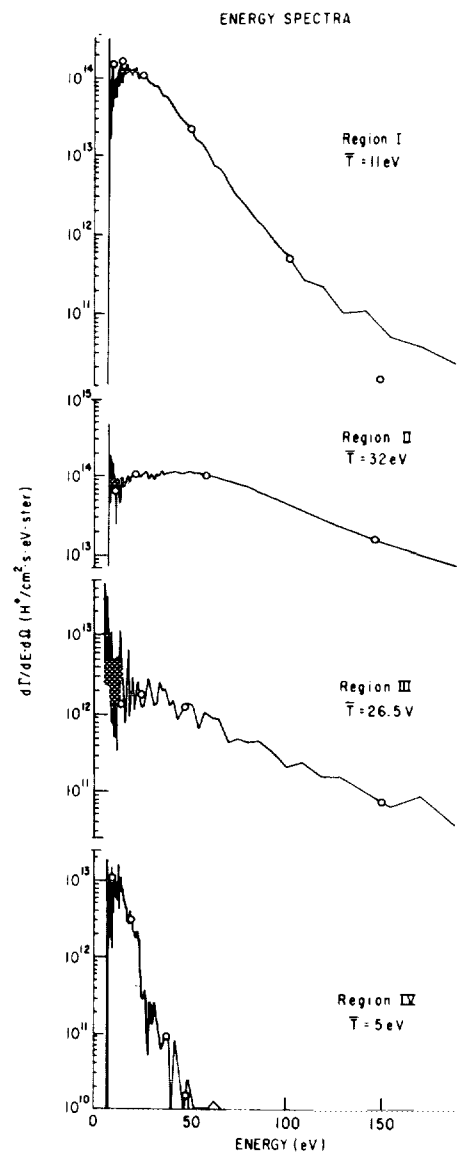


FIG. 2. Energy spectra of H^0 emitted during high ionization PDC from a clean PLT for each of the four regions shown in Fig. 1. The dots represent Maxwellian distributions at the stated temperatures \bar{T} . Note the differing ordinate for each region.

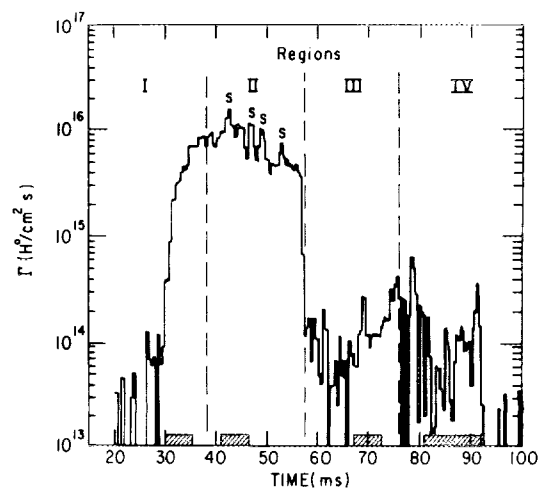


FIG. 3. Total efflux (Γ) of H^0 's between 7.0 and 405 eV vs time for the same discharge detailed in Fig. 1. The peaks marked with an "S" are in phase with increased O and C in the plasma, measured spectroscopically.

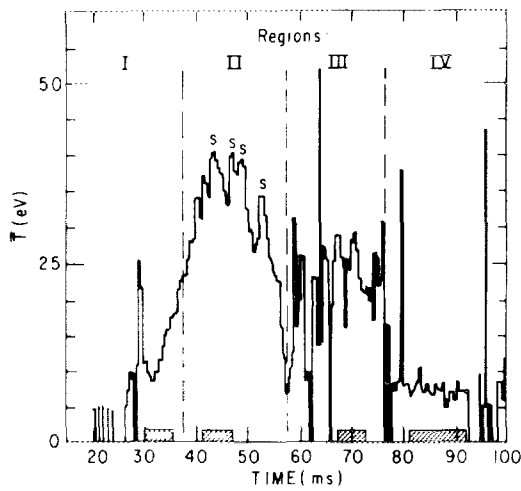


FIG. 4. Line averaged ion temperature (\bar{T}) vs time for the same discharge detailed in Fig. 1. The peaks marked with an "S" coincide with those marked in Fig. 3.

$$\Gamma = \int_0^{2a} n_{H^0} n_H \cdot \langle \sigma v \rangle_{cx} \exp\left(-\int_0^x \frac{dx'}{\lambda}\right) dx, \quad (2)$$

where

$$\lambda = V_{H^0} / n_e \langle \sigma v \rangle_{ion},$$

the mean free path for ionization,

V_{H^0}	= velocity of H^0 ,
$\langle \sigma v \rangle_{cx}$	= charge exchange rate coefficient,
$\langle \sigma v \rangle_{ion}$	= electron impact rate coefficient,
n_i	= density of the i th species,
a	= minor radius of the tokamak, and
x	= distance along detector line-of-sight from outer wall.

For all of the PDC discharges, the low density and low temperature allow $\lambda \gtrsim a$, i.e., the plasma is transparent to the neutrals. Thus the temperature determined from $d\Gamma/dE$ is a line average ion temperature \bar{T} representative of the entire plasma. Figure 4 shows \bar{T} as a function of time. It is calculated from the average energy E_{av} since, for a Maxwellian distribution $E_{av} = 2T$.

Region I of the pulsed discharge is similar to startup of a normal tokamak discharge. Flux and \bar{n}_e rise simultaneously and are near the same levels as in a normal discharge. The simultaneous rise is expected because of Γ 's direct dependence on n_H . The flux and ion temperature attained, $10^{16} H^0/cm^2 \cdot s$ at 30 eV, are sufficient to cause CO and CH₄ desorption¹⁰ equal to the CO and CH₄ measured by RGA in the vacuum vessel after the pulse. However ionization of these molecules during the pulse may occur and thus another mechanism may be responsible for the CO and CH₄ eventually pumped away. The platinum bolometer also sees the same level of radiated power, $\sim 3 W/cm^2$, as in a normal discharge. Spectroscopic measurements showed the presence of OV. This indicates an electron temperature in excess of ~ 20 eV. The 10% rise in duct pressure in region I is presumably the result of a $\sim 50\%$ rise in vessel pressure due to desorption of gas from the wall. Throughout regions I and II, \bar{T} follows the input power $I_p V_L$.

In region II, Γ and \bar{T} show in-phase large-scale fluctuations. Four of these peaks are marked with an "S" on Figs. 3 and 4. At these points sputtering and desorption from the wall are calculated to be enhanced by at least a factor of 10. Spectroscopic measurements during these peaks show large increases in O and C light. These fluctuations probably arise from large-scale plasma instabilities which cause increased plasma contact with the wall. They may therefore be important to the cleaning process.

Region III is characterized by \bar{n}_e and I_p having near zero values. The input power $I_p V_L$ is about 10^{-2} of its value during region II; so Γ appears proportional to the input power. At this low I_p , charged particle lifetimes due to grad B and curvature drifts are estimated to be ~ 10 ms for 30 eV particles. When the plasma again breaks down to start region IV, the lack of primary-induced V_L means less input power. Accordingly the T_i and Γ are much lower.

All the aforementioned results apply to PDC in a clean environment at $P_{fill} \sim P_c$. Some significant changes in plasma behavior result at lower P_{fill} and in dirtier environments. In a clean machine the magnitude of Γ and \bar{T} in regions III and IV falls as P_{fill} is lowered. At the lower P_{fill} region III still exists but region IV is absent. In a dirty machine the Γ and \bar{T} of region IV also fall and then disappear as P_{fill} is lowered from P_c , but they fall from a higher level. In a dirty machine Γ and \bar{T} in region IV equal that of region II at $P_{fill} = P_c$. Region III behaves differently in the dirty machine. It only exists at the lower fill pressures.

Independent of P_{fill} , \bar{T} of a dirty machine only reaches a maximum of ~ 15 eV—about half the value of the clean case. Also, regardless of P_{fill} in a dirty machine, region II ends when $V_L = 0$. In the very dirty case (the first 5000 discharges after opening) this lack of I_p -induced V_L goes even further: region IV (a second current and density bump) starts before V_L drops, and ends abruptly when I_{OH} returns to zero. As the machine cleans up, first region IV extends past $I_{OH} = 0$ and then region II expands past the $V_L = 0$ point.

V. LOW IONIZATION PDC

When the fill pressure is raised above P_c the discharge abruptly changes to the low ionization type. The P , \bar{n}_e , I_p , and Γ for this type of discharge in a clean air machine are shown in Fig. 5. The results are similar in a dirty machine. The pressure reaches a minimum of only 3.2×10^{-4} Torr at 0.15 s. Unlike the high ionization case, the pressure rose at each flux peak, indicating more gas desorption.

The amount of CH₄ produced by these discharges was about 1/3 that of the high ionization case. However, no measurable C II emission came from the plasma indicating either $T_e \lesssim 3$ eV or methane generation subsequent to the discharge. From the rate of rise of electron density $T_e \simeq 3$ eV is also estimated.

The flux measured during these discharges, $5 \times 10^{13}/cm^2 \cdot s$ with $\bar{T} \sim 20$ eV, is at least 100 times less than would be expected if the bulk of the protons had $T \sim 20$ eV and charge exchanged with molecular hydrogen.¹¹ Therefore the 20-eV distribution observed must be a small fraction of the main proton distribution. The temperature of the main distribution is probably latched to T_e because of the rapid equilibra-

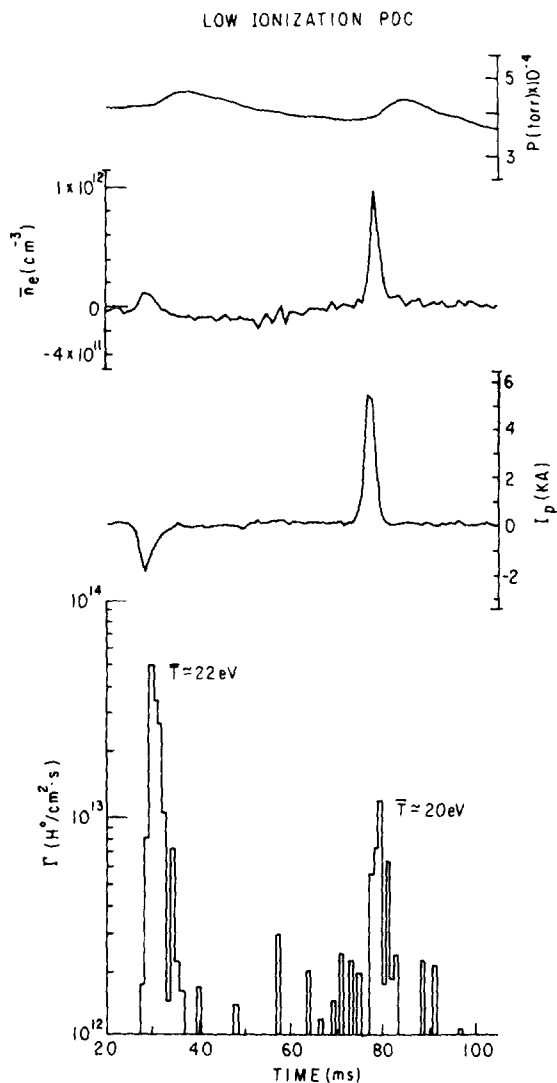


FIG. 5. P , \bar{n}_e , I_p , and Γ for low ionization PDC in a clean PLT. The I_{OH} , V_L , and TF were the same as those during the high ionization PDC shown in Fig. 1. The \bar{T} 's indicated on the figure are for the flux of H^0 with $E > 7.0$ eV.

tion time, which is 1 ms at $T_e = 3$ eV. Measurements of T_i on Alcator¹² during Taylor discharge cleaning do show a neutral temperature of ~ 3 eV. The energetic 20-eV-proton tail

could be produced by an energetic electron tail causing a plasma instability.

The fluence per pulse, $F = \int \Gamma(t) dt$, in the energy range 7 to 400 eV is $1.3 \times 10^{11}/\text{cm}^2$ for these low ionization discharges and $4 \times 10^{14}/\text{cm}^2$ for the high ionization discharges. Therefore methane formation does not simply depend on the fluence of "energetic," $E > 5$ eV hydrogen. Possibly ionization of carbon and oxygen molecules are important¹³ or 3 eV H^0 are sufficient for carbon removal.

VI. SUMMARY

The time-resolved neutral efflux with energy between 7 and 1000 eV has been measured during high and low ionization modes of pulsed discharge cleaning on PLT. The high ionization mode is characterized by $\sim 10^{16} H^0/\text{cm}^2\cdot\text{s}$ with an ion temperature of 20 to 30 eV. The low ionization mode has a 1000 times lower fluence in the same energy range (7 to 1000 eV). A bulk temperature of ~ 3 eV for the low ionization mode is inferred. Methane production was comparable in both modes of operation.

Supported by the U. S. Department of Energy Contract No. DE-AC02-76-CHO3073 and the Fannie and John Hertz Foundation.

¹H. F. Dylla, *J. Nucl. Mater.* **93&94**, 61 (1980).

²R. J. Taylor, *J. Nucl. Mater.* **76&77**, 41 (1978).

³H. F. Dylla, K. Bol, S. A. Cohen, R. J. Hawryluk, E. B. Meservey, and S. M. Rossmagel, *J. Vac. Sci. Technol.* **16**, 752 (1979).

⁴S. Suckewer (private communication).

⁵D. E. Voss and S. A. Cohen, *Rev. Sci. Instrum.* **53**, 1696 (1982).

⁶D. Ruzic and S. Cohen, PPPL report (to be published).

⁷E. Hinnov and F. W. Hofmann, *J. Opt. Soc. Am.* **53**, 1259 (1963).

⁸J. Schivell, G. Renda, J. Lowrance, and H. Hsuan, *Rev. Sci. Instrum.* **53**, 1527 (1982).

⁹P. Schmidlin, H. E. Zuvers, and G. E. Oliaro, in *Proceedings of the 8th IEEE Symposium on Engineering Problems of Fusion Research* (San Francisco, California, 1979), Vol. IV, p. 2192.

¹⁰G. Farrell and B. D. Eghawary, *J. Nucl. Mater.* **93&94**, 834 (1980).

¹¹The charge exchange flux may originate from $H^+ - H^0$ collisions or $H^+ - H_2$ collisions. The first case has a higher rate coefficient by a factor of 100. Thus by assuming that only H^+ and H_2 exist in the plasma, a lower limit on the expected flux is predicted.

¹²E. S. Marmor (private communication).

¹³L. Oren and R. J. Taylor, *Nucl. Fusion* **17**, 1143 (1977).